

# 717-mV open-circuit voltage silicon solar cells using hole-constrained surface passivation

J. Zhao, A. Wang, A. Aberle, S. R. Wenham, and M. A. Green  
*Centre for Photovoltaic Devices and Systems, University of New South Wales, Kensington, Australia 2033*

(Received 4 September 1992; accepted for publication 2 November 1993)

A virtual saturation of the supply of holes leading to an injection level dependent reduction in surface recombination velocity has been shown to be responsible for the improved performance of recent high efficiency silicon solar cells. By fabricating test cells taking advantage of this and other recombination reduction mechanisms, improved open-circuit voltages of 717 mV have been independently confirmed for experimental silicon cells. These voltages correspond to saturation current densities of  $25 \text{ fA/cm}^2$  at  $25^\circ\text{C}$ , also the lowest demonstrated for a silicon junction device. Further improvement in both voltage and cell efficiency is expected to result from this work.

The passivated emitter, rear locally diffused (PERL) solar cell structure of Fig. 1(a) has resulted in markedly improved efficiency for silicon solar cells.<sup>1,2</sup> Under the standard global Air Mass 1.5 spectrum normalized to  $100 \text{ mW/cm}^2$  at  $25^\circ\text{C}$ , these cells demonstrate energy conversion efficiencies about 23% with typical open-circuit voltages of 700 mV, short-circuit current densities of  $41 \text{ mA/cm}^2$  and fill factors of 81%.<sup>2</sup> This improved performance results largely from the high levels of passivation of the rear of the cell at operating voltages. This passivation is shown to be due to a suppression of rear surface recombination induced at operating voltages by constraints upon the capture of holes by surface interface levels. Building on this knowledge, improved open-circuit voltage has been demonstrate in silicon cells in streamlined test cell structures as shown in Fig. 1(b) Such improved open-circuit voltage historically has been a precursor to improved cell efficiency.

Figure 2 (solid line) shows the dark current-voltage characteristics of a 22.9% efficient PERL cell ( $1\text{-}\Omega \text{ cm}$  substrate resistivity). At low current, these characteristics can be fitted<sup>3</sup> by an exponential (a straight line on the semilogarithmic plot) corresponding to a diode ideality factor<sup>4</sup> of unity and a saturation current density of  $1050 \text{ fA/cm}^2$  (zero voltage intercept). At about 0.45-V bias, there is departure from this ideal behavior. Above about 0.6-V bias, the curve can be fitted by another linear segment with unity ideality factor corresponding to a much lower saturation current density of  $62 \text{ fA/cm}^2$ , when the effect of a cell series resistance of  $0.2 \Omega \text{ cm}^2$  is taken into account.

This unusual characteristic can be explained by considering recombination at the oxidized rear surface of the cell.<sup>5</sup> With small voltages across the cell, noncontacted regions of the rear surface are weakly depleted due to the combination of the effects of positive oxide charges and the work function of the overlying rear metal (Al). Recombination rates are high. Cell characteristics then approach those of devices with infinite rear surface recombination velocities. The saturation current density of  $1050 \text{ fA/cm}^2$  deduced at such bias corresponds to that expected under these conditions using newly measured values of the silicon intrinsic carrier

concentration.<sup>6</sup> (Since the saturation current density depends upon the square of this concentration,<sup>4</sup> the new values predict a current density about half that calculated using older values.) As the voltage across the cell increases, the hole concentration at the rear increases only marginally while the electron concentration increases approximately exponentially.<sup>5</sup> Since the capture cross section of surface states for electrons is found to be much larger than that for

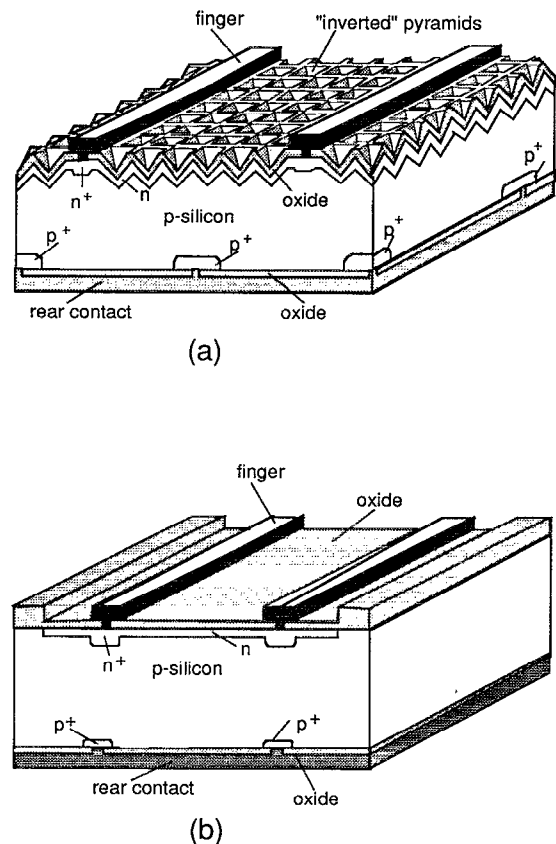


FIG. 1. (a) PERL cell (passivated emitter rear locally diffused); (b) streamlined PERL test structure used for present measurements.

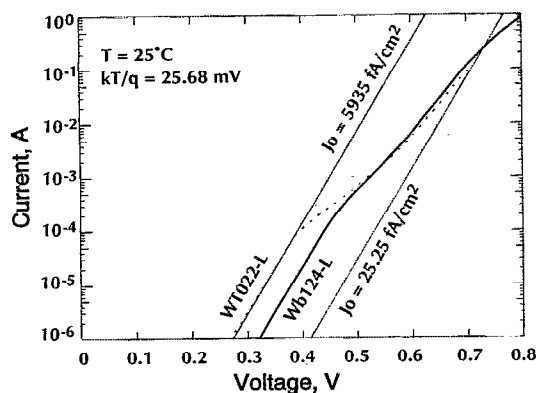


FIG. 2. Dark current-voltage characteristics of a 1- $\Omega$  cm, 280- $\mu$ m-thick 22.9% efficient PERL cell as measured at Sandia National Laboratories (solid line) compared to those for a 2.5- $\Omega$  cm, 185- $\mu$ m-thick PERL-test structure (dashed line).

holes for high quality oxides,<sup>7-9</sup> the rate of hole capture becomes the rate limiting process for recombination along the rear. Because the rear hole concentration is not a strong function of cell voltage, the recombination rate virtually saturates. This results in a surface recombination velocity which decreases approximately exponentially with increasing injection level, since this velocity is referenced to the increasing bulk electron concentration. Calculations based on the current-voltage curve shown show that the recombination velocity decreases from 15 000 cm/s at 0.45-V bias to below 50 cm/s at 0.65-V bias.<sup>10</sup> The reduced recombination velocity decreases the dark saturation current density of the diode over the 0.45–0.60 V region in Fig. 2 as per standard diode theory.<sup>4</sup> At higher voltages, recombination in the diffused regions along the top surface of the cell become more important, introducing the second linear component to the curve.

With this improved knowledge of cell operation, test cell structures as shown in Fig. 1(b) were fabricated to demonstrate improved open-circuit voltage. This requires a reduction in all processes likely to contribute to the recombination of photogenerated carriers when the cell is open circuited. There are three main modifications from the normal structure of Fig. 1(a). One is the use of a planar <100> orientated top surface. This reduces the area of the diffused emitter, reducing both its volume and the total number of interface states, and hence the contribution of the emitter and top surface to recombination. The second is the growth of a higher quality oxide along the rear surface and in the periphery of the test device. It was found empirically that growing the oxide in dry oxygen with 1% trichloroethane, as for standard PERL cells, but for a more prolonged growth period of 15 h (8000-Å initial oxide thickness) gave best results. This may be due to reduced interface state densities or capture cross sections, with midgap state densities well below  $10^{10}$  cm<sup>-2</sup> eV<sup>-1</sup> measured for similarly grown oxides.<sup>11</sup> This is comparable to a very good quality, microelectronics-grade oxide.

The surface of the *p*-type silicon which is overlain by oxide both around the periphery of the cell on the top surface and along the rear is weakly depleted at low voltage bias

TABLE I. Performances on planar PERL cell WT022-L measured at Sandia National Laboratories under global AM1.5 spectrum normalized to 100 mW/cm<sup>2</sup> at 25 °C.  $V_{OC}$  is open circuit voltage,  $J_{SC}$  is short circuit current density, and FF is fill factor.

Condition	$V_{OC}$ (mV)	$J_{SC}$ (mA/cm <sup>2</sup> )	FF (%)	Efficiency (%)
Whole wafer	717	9.1	78.5	5.2
Periphery shaded	710	33.3	80.6	19.0

and, hence, has poor recombination velocities. At operating voltages, the previous hole-constrained effect reduces these recombination velocities to low levels not only along the rear surface, but in the unmetallized peripheral regions of the top surface as demonstrated experimentally elsewhere.<sup>8,9</sup> These effects are further enhanced in the present devices by the high growth temperatures and times of the oxide previously mentioned. This depletes boron from the cell surface which further constrains the capture of holes by interface levels. The third modification is that the substrate for the test structure is thinned to 185  $\mu$ m to reduce the bulk contribution to recombination. The cells were tested under the standard global Air Mass 1.5 spectrum at Sandia National Laboratories with the results listed in Table I.

When tested unmasked and unscribed from the 5-cm-diam wafer in which they were fabricated, the cells demonstrated open-circuit voltages of up to 717 mV. This is the highest value ever reported for a silicon device under standard test conditions. [An earlier reported value of 720 mV for a device relying on SIPOS, semi-insulating polysilicon, passivation was measured at 130-mW/cm<sup>2</sup> light intensity (Ref. 12), corresponding to an estimated voltage of 712 mV under standard test conditions.] Based on the total wafer area, the efficiency of this device is quite modest as shown. With the cell masked through a 2 cm $\times$ 2 cm mask so that only the top diffused area is illuminated, an improved efficiency was noted but with a reduction of open-circuit voltage. The difference between masked and unmasked results suggests that total recombination rates are lower in peripheral regions than in the main cell area. When the cell is open circuited and the device unmasked, carriers in excess of those required to satisfy recombination in peripheral regions flow to the main cell. However, when masked, some of the photogenerated carriers in the main cell region have to flow in the opposite direction to recombine in peripheral regions, reducing the open-circuit voltage.

The dark current-voltage characteristics of the 2.5- $\Omega$  cm cells are also shown in Fig. 2 (dotted line). At low currents, an exponential region is again observed corresponding to a dark saturation current density of 5900 fA/cm<sup>2</sup>. This is higher than observed with the standard PERL cell due to the lighter doping in the substrate and its reduced thickness. At higher current densities, another linear region can be identified when allowance is made for series resistance. The saturation current density of 25.3 fA/cm<sup>2</sup> for this region was deduced by comparing the dark current-voltage curves with illuminated open-circuit voltage versus short-circuit current characteristics. At intermediate current levels, there is con-

siderable overlap between the dark current-voltage curve of this and the standard PERL device.

Interpreting these results on same basis as before, the overlap at intermediate current levels implies a lower rear surface recombination velocity for a given bias by a factor of about 2.5 corresponding to the lower doping level. The reduced saturation current density at high current levels, also by a factor of about 2.5, is attributed to reduced recombination in the emitter region. As previously noted, the reduced emitter recombination current arises from the decrease volume of  $n$ -type diffusion and its reduced surface area, both due to the use of a planar structure, and the lower interface state densities along this region due to its  $\langle 100 \rangle$  orientation.

Current work is following two parallel strands to take advantage of these improvements. Special test structures are being developed to further reduce the dominant contributors to saturation current density identified above. These devices may result in further improvements to cell open-circuit voltage. Modifications to the high efficiency structure of Fig. 1(a) are also being implemented to allow these open-circuit voltage improvements to be incorporated into high efficiency devices.

The authors gratefully acknowledge the contributions of other members of the Centre for Photovoltaic Devices and Systems, particularly A. Sproul for his contributions to the interpretation of these results. Portions of this work were supported by the Energy Research and Development Corpo-

ration, the Australian Research Council and Sandia National Laboratories. The Centre for Photovoltaic Devices and Systems is supported by the Australian Research Council Special Research Centres Scheme and Pacific Power.

<sup>1</sup>A. Wang, J. Zhao, and M. A. Green, *Appl. Phys. Lett.* **57**, 602 (1990).

<sup>2</sup>M. A. Green, in *Proceedings of the 10th European Communities Photovoltaic Solar Energy Conference*, Lisbon, (Kluwer, Dordrecht, 1991), pp. 250–253.

<sup>3</sup>We are grateful to P. Basore from Sandia National Laboratories, Albuquerque, NM, for this observation.

<sup>4</sup>Martin A. Green, *Solar Cells: Operating Principles, Technology and System Applications* (Prentice-Hall, Englewood Cliffs, 1982) (Reprinted 1986, 1992).

<sup>5</sup>M. A. Green, A. W. Blakers, J. Zhao, A. Wang, A. M. Milne, X. Dai, and C. M. Chong, "High Efficiency Silicon Concentrator Solar Cell Research," Report No. SAND89-7041, Sandia National Laboratories, New Mexico 1989.

<sup>6</sup>A. B. Sproul and M. A. Green, *J. Appl. Phys.* **70**, 846 (1991).

<sup>7</sup>W. D. Eades and R. M. Swanson, *J. Appl. Phys.* **58**, 4267 (1985).

<sup>8</sup>A. Aberle, Ph.D. thesis, Albert-Ludwigs-University, Freiburg, 1991 (in German).

<sup>9</sup>A. Aberle, S. Glunz, and W. Warta, *J. Appl. Phys.* **71**, 4422 (1992).

<sup>10</sup>M. A. Green, S. R. Wenham, J. Zhao, A. Wang, X. Dai, A. Milne, M. Taouk, J. Shi, F. Yun, B. Chan, A. B. Sproul, and A. Stephens, "One-Sun Silicon Solar Cell Research" Sandia Contractor Report No. SAND92-7013, January, 1993.

<sup>11</sup>S. Glunz, Fraunhofer Institute for Solar Energy Systems (private communication).

<sup>12</sup>E. Yablonovitch, R. M. Swanson, and Y. H. Kwark, in the Conference Record of the 17th IEEE Photovoltaic Specialists Conference, Kissimmee, FL, 1984 (unpublished), p. 1146.